Journal of Anatomy

J. Anat. (2009) **214**, pp245–257 doi: 10.1111/j.1469-7580.2008.01028.x

Dual role for neural crest cells during outflow tract septation in the neural crest-deficient mutant *Splotch^{2H}*

Lucy Bradshaw,[1] Bill Chaudhry,[1] Victoria Hildreth,[1] Sandra Webb[2] and Deborah J. Henderson[1]

[1]*Institute of Human Genetics, Newcastle University, Newcastle upon Tyne, UK*
[2]*Basic Medical Sciences, Developmental & Endocrine Signalling, St George's University of London, London, UK*

Abstract

Splotch^{2H} (*Sp^{2H}*) is a well-recognized mouse model of neural crest cell (NCC) deficiency that develops a spectrum of cardiac outflow tract malformations including common arterial trunk, double outlet right ventricle, ventricular septal defects and pharyngeal arch artery patterning defects, as well as defects in other neural-crest derived organ systems. These defects have been ascribed to reduced NCC in the pharyngeal and outflow regions. Here we provide a detailed map of NCC within the pharyngeal arches and outflow tract of *Sp^{2H}*/*Sp^{2H}* embryos and fetuses, relating this to the development of the abnormal anatomy of these structures. In the majority of *Sp^{2H}*/*Sp^{2H}* embryos we show that deficiency of NCC in the pharyngeal region results in a failure to stabilize, and early loss of, posterior pharyngeal arch arteries. Furthermore, marked reduction in the NCC-derived mesenchyme in the dorsal wall of the aortic sac disrupts fusion with the distal outflow tract cushions, preventing the initiation of outflow tract septation and resulting in common arterial trunk. In around 25% of *Sp^{2H}*/*Sp^{2H}* embryos, posterior arch arteries are stabilized and fusion occurs between the dorsal wall of the aortic sac and the outflow cushions, initiating outflow tract septation; these embryos develop double outlet right ventricle. Thus, NCC are required in the pharyngeal region both for stabilization of posterior arch arteries and initiation of outflow tract septation. Loss of NCC also disrupts the distribution of second heart field cells in the pharyngeal and outflow regions. These secondary effects of NCC deficiency likely contribute to the overall outflow phenotype, suggesting that disrupted interactions between these two cell types may underlie many common outflow defects.

Key words heart; neural crest cells; second heart field; *Splotch^{2H}*; outflow tract; pharyngeal arch arteries.

Introduction

Formation of the pharyngeal arch arteries and septation of the outflow tract into the distinct vessels of the aorta and pulmonary trunk involves three major components: endocardial-derived cells (Bernanke & Markwald, 1982), cardiac neural crest cells (NCC; Kirby et al. 1983) and cells originating in the second (or anterior) heart field (SHF; Kelly et al. 2001; Mjaatvedt et al. 2001; Waldo et al. 2001). Cells of endocardial origin form the endothelial lining of the vessels and also transform into mesenchyme to contribute to the more proximal regions of the outflow tract cushions (Lincoln et al. 2004), from which the valves form. NCC, originating in the dorsal part of the neural tube, migrate through the pharyngeal arches where they stabilize the nascent arch arteries, and then continue onwards to fill the outflow tract cushions (Kirby et al. 1983; Jiang et al. 2000). Loss or deficiency of NCC is associated with outflow tract septation defects including common arterial trunk (Kirby et al. 1983), suggesting NCC play a major role in this process. More recently, it has been shown that SHF cells, as well as forming the outflow tract myocardium and the smooth muscle of the distal outflow tract (Waldo et al. 2005a,b) are also essential for normal outflow tract septation (Xu et al. 2004), although their precise role(s) in this process remain unclear.

Although the mechanism underlying cardiac outflow septation remains controversial, the structure often referred to as the aorto-pulmonary (AP) septum has been suggested to play key roles during separation of the initially single outflow vessel to form the ascending aorta and the pulmonary trunk (Bartelings & Gittenberger-de Groot, 1989; Icardo, 1990; Webb et al. 2003). The septum corresponds to the dorsal wall of the aortic sac which separates the origins of the 4th and 6th aortic arch arteries. Fusion of the septum with the distal outflow cushions, as a consequence of the extensive remodelling that takes place in the pharyngeal region, initiates outflow tract septation. Septation then proceeds in a distal to proximal wave through the outflow tract (Hutson & Kirby, 2007). In this way, the aortic blood

Correspondence
Dr Deborah Henderson, Institute of Human Genetics, Newcastle University, Newcastle upon Tyne, NE1 3BZ, UK.
T: +44 191 2418644; F: +44 191 2418666; E: D.J.Henderson@ncl.ac.uk

Accepted for publication *14 November 2008*

flow within the outflow tract exits via the arteries of the 4th aortic arches, whilst the pulmonary flow exits via the 6th arch arteries and into the developing pulmonary arteries; asymmetrical remodelling results in a left-dominant aortic arch system in mammals. Finally, fusion of the proximal outflow cushions with the atrio-ventricular cushions where they span the ventricular septum closes the inter-ventricular foramen, thus completing not only septation of the outflow tracts, but also septation of the ventricles. Although the embryological processes underlying outflow tract septation are becoming elucidated, the relative importance of the different cell types which are found within the pharyngeal and outflow regions as septation is underway, remain unclear.

The *splotch* mouse mutant is a recognized model of NCC deficiency (Franz, 1989; Conway et al. 1997a) caused by mutations in the *Pax3* gene. The Sp^{2H} allele (Beechey & Searle, 1986) has a 32-base pair deletion within the homeobox, which results in a premature stop codon and production of a truncated, non-functional protein (Epstein et al. 1991). Sp^{2H}/Sp^{2H} embryos have a range of malformations including neural tube defects, muscle migration defects and abnormalities in NCC-derived structures. Defects in the developing cardiac outflow tract, including common arterial trunk, double outlet right ventricle and associated aortic arch and ventricular septation defects (Franz, 1989; Conway et al. 1997a) have been linked to a reduction in NCC in the pharyngeal arches and outflow tract (Conway et al. 1997b, 2000; Epstein et al. 2000; Chan et al. 2004). However, none of these studies has mapped the NCC in relation to the development of the abnormal anatomy in the outflow region, a process that is crucial for understanding how the deficiency in NCC might result in outflow defects.

In this study, we begin to elaborate how the deficiency of NCC in both the pharyngeal arches and the outflow tract result in outflow tract defects. Furthermore, we show that deficiency of NCC disrupts SHF cells within the walls of the aortic sac and outflow tract, potentially exacerbating the effects of loss of NCC alone.

Materials and methods

Mice and embryos

$Splotch^{2H}$ mice were obtained from Prof. Andrew Copp (University College London). Male and female Sp^{2H}/+ mice (Beechey & Searle, 1986) were mated overnight to generate timed pregnancies. The genotype of embryos was assessed by PCR as described (Epstein et al. 1991). *Wnt1*-Cre (Danielian et al. 1998) and *ROSA 26R* (Soriano, 1999) mice were obtained from Prof. Shoumo Bhattacharya (Oxford, UK). Sp^{2H} females were inter-crossed with both *Wnt1*-Cre and *ROSA 26R* males to produce separate lines. Sp^{2H}; *Wnt1*-Cre and Sp^{2H}; *ROSA 26R* animals were then inter-crossed to produce litters in which the offspring carried the Sp^{2H} mutation together with the *Wnt1*-Cre and *ROSA 26R* transgenes. Careful analysis of more than 30 Sp^{2H}/Sp^{2H}; *Wnt1*-Cre; *ROSA 26R* embryos and fetuses suggested that there were no significant changes in the Sp^{2H}/Sp^{2H} cardiac phenotype as a consequence of being inter-crossed with the *Wnt1*-Cre and *ROSA 26R* lines. Embryos were dissected, fixed and prepared either for Xgal staining (Jiang et al. 2000) or for embedding in paraffin wax as described previously (Henderson et al. 1999). At least three embryos of each genotype were examined at each gestational age studied. Sp^{2H}/+ embryos were routinely used as normal controls as in over 200 embryos examined to date, no cardiac defects have been observed.

Histology and immunohistochemistry

Immunohistochemistry and Xgal staining were carried out as described previously (Henderson et al. 1999; Loughna & Henderson, 2007). The anti-Isl1 and MF20 antibodies were obtained from the Developmental Studies Hybridoma Bank (University of Iowa), and the anti α-smooth muscle actin antibody (αSMA; clone 1A1) was obtained from Sigma. Staining for elastic fibres was performed using Miller's elastin stain. Antibody-stained and Miller's elastin-stained sections were counterstained with methyl green. Xgal-stained sections were counterstained with 1% eosin. Images were captured on a Zeiss Axiophot II microscope using a digital camera.

3D reconstruction

Serial sagittal sections (8 μm) were collected from E10.5 Sp^{2H}/+ and Sp^{2H}/Sp^{2H} embryos and photographed using a digital camera. Reconstruction was carried out using AMIRA (Mercury) software.

Proliferation index of NCC in the outflow cushions

pHH3 staining was carried out on three Sp^{2H}/Sp^{2H} embryos and three stage-matched controls. The total number of cells was counted from alternate sections passing through the outflow cushions. In addition, pHH3-positive cells were counted in each case to calculate a proliferation index. A total of 2663 cells were counted from Sp^{2H}/+ embryos, compared with 1404 from Sp^{2H}/Sp^{2H} embryos, reflecting the NCC deficiency in the Sp^{2H}/Sp^{2H} embryos. Statistical significance was determined using the Chi-squared test.

Results

Marked deficiency of NCC in the pharyngeal and outflow regions in Sp^{2H}/Sp^{2H} embryos

Hypoplastic pharyngeal arches 3–6, associated with deficiency of NCC in the outflow tract (Fig. 1A,B), have been described previously in *Splotch* embryos (Epstein et al. 2000). Sectioning of these embryos confirmed these findings and clarified how deficiency of NCC related to the morphology of the pharyngeal and cardiac outflow regions.

NCC, expressing βgal, were abundant in the pharyngeal region of the control embryo, entirely filling the region between the foregut and the dorsal wall of the aortic sac (black arrows in Fig. 1C), including the region of the dorsal wall that will later fuse with the distal outflow cushions to initiate outflow septation (arrowhead in Fig. 1C). In

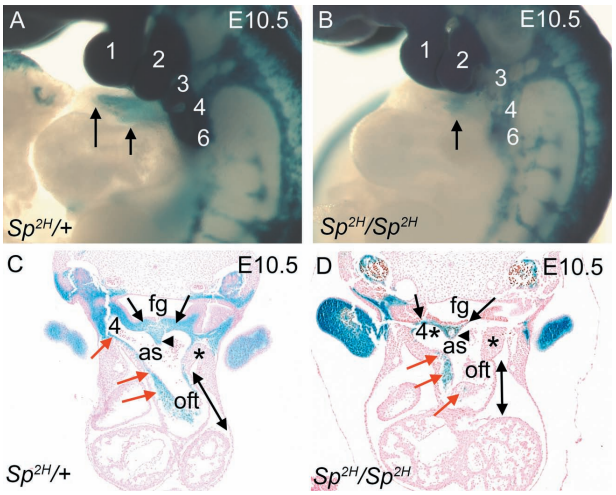

Fig. 1 NCC distribution in the pharyngeal and outflow regions of Sp^{2H} embryos at E10.5, before outflow tract septation. (A,B) βgal-stained NCC, viewed in whole E10.5 embryos, populate the pharyngeal arches (numbered 1–6) and the outflow tract (arrows) in Sp^{2H}/+ embryos (A). In contrast, although NCC are abundant in the 1st and 2nd pharyngeal arches in Sp^{2H}/Sp^{2H} embryos, they are markedly deficient in the posterior arches 3–6 and do not penetrate as far into the outflow tract in Sp^{2H}/Sp^{2H} embryos (arrow in B). (C,D) Sectioning of embryos reveals that NCC are abundant in the mesenchyme of the pharyngeal arches and in the dorsal wall of the aortic sac (black arrows in C), including the region between the 4th and 6th arches (arrowhead in C). NCC are also continuous through the walls of the aortic sac and into the outflow cushions (red arrows in C). NCC are markedly deficient in the pharyngeal region of Sp^{2H}/Sp^{2H} embryos, which results in a marked reduction in the amount of mesenchyme present. As a consequence, the dorsal wall of the aortic sac is markedly thinned (black arrows in D), altering the architecture of the aortic sac. There are also reduced numbers of NCC in the outflow cushions (red arrows in D). The lateral walls of the aortic sac are thickened in Sp^{2H}/Sp^{2H} embryos compared with Sp^{2H}/+ littermates (asterisks). The outflow tract also appeared shortened in Sp^{2H}/Sp^{2H} embryos, compared with Sp^{2H}/+ littermates (compare length of double-headed arrows in C,D). as, aortic sac; fg, foregut; oft, outflow tract.

contrast, much of the pharyngeal region lacked βgal staining and there was a marked reduction in tissue between the foregut and the dorsal wall of the aortic sac in the majority of the Sp^{2H}/Sp^{2H} embryos (black arrows in Fig. 1D), including the region between the origins of the 4th and 6th pharyngeal arch arteries (black arrowhead in Fig. 1D). Although it was not possible to be sure which Sp^{2H}/Sp^{2H} embryos would develop common arterial trunk, compared with those that would develop double outlet right ventricle, at this early stage of development all of the embryos examined at E10.5 ($n > 20$) manifested the thinned region between the dorsal wall of the aortic sac and the foregut, although it did vary somewhat in extent. The outflow tract appeared shortened in Sp^{2H}/Sp^{2H} embryos compared with control littermates (double-headed arrows in Fig. 1C,D) and the mesenchyme at the lateral sides of the aortic sac was thickened (asterisks in Fig. 1C,D). These abnormalities have not been previously reported in Sp^{2H}/Sp^{2H} embryos, although they have been described in chicken embryos in which cardiac NCC were ablated (Waldo et al. 2005a).

Examination of sagittal sections demonstrated the extensive NCC contribution to the mesenchyme of the pharyngeal arches in control embryos (Fig. 2A,C,E and Supplementary Fig. 1). This contrasted with the dramatic reduction in the numbers of βgal-stained cells in the 3rd, 4th and 6th pharyngeal arches in Sp^{2H}/Sp^{2H} embryos. Thus pharyngeal arches 3, 4 and 6 appeared hypoplastic and the region between the dorsal wall of the aortic sac and the foregut was thinned and acellular, with little βgal staining.

In addition to these abnormalities within the pharyngeal region and the aortic sac, there was also a marked reduction in the number of NCC found within the outflow tract cushions in all of the Sp^{2H}/Sp^{2H} embryos examined (red arrows in Fig. 1D). Proliferating cells, marked by their expression of pHH3, were apparent within the outflow tract cushions (Supplementary Fig. 2A,B). Counting of the pHH3-positive cells within the outflow tract cushions at E10.5 showed that there was no statistical difference in the mitotic index between Sp^{2H}/+ and Sp^{2H}/Sp^{2H} embryos (MI = 3.1% in both cases). Moreover, cell death analyses showed little or no cell death in the outflow cushions at this stage (Supplementary Fig. 2C,D). Together, these data suggest that the hypoplastic outflow cushions seen later in development in Sp^{2H}/Sp^{2H} (Figs 3 and 4) are likely to result from the reduced numbers of NCC migrating into the outflow region, rather than from abnormalities in proliferation or cell death after their colonization of the cushions.

Abnormal patterning of posterior pharyngeal arch arteries in Sp^{2H}/Sp^{2H} embryos

Pharyngeal arch patterning defects have been described previously in the *Splotch* mutant (Franz et al. 1989), although the aetiology was not analysed. We therefore examined the development of the pharyngeal arch arteries in closer detail and found that the 1st and 2nd pharyngeal arch arteries, which appear earlier than the more posterior vessels, had formed normally in Sp^{2H}/Sp^{2H} embryo control littermates (data not shown), as expected by the normal NCC contribution to these arches. At E10.5, the forming arch arteries were completely embedded in NCC-derived tissue and each could be seen to connect proximally to the aortic sac and distally to the descending aorta on both right and left sides (Fig. 2A,C,E and data not shown). The 3rd and 4th pharyngeal arch vessels had a similar-sized lumen, whereas the 6th arch artery was narrower at this stage. Examination of stage-matched Sp^{2H}/Sp^{2H} embryos revealed abnormalities in the posterior pharyngeal arch arteries seen as early as E10.5, shortly after they first appear, in the majority of cases. Although vessels could be seen within the 4th and 6th pharyngeal arches, one or both were frequently hypoplastic and non-patent (Fig. 2B,D,F), whilst the 3rd pharyngeal arch artery was dilated in the

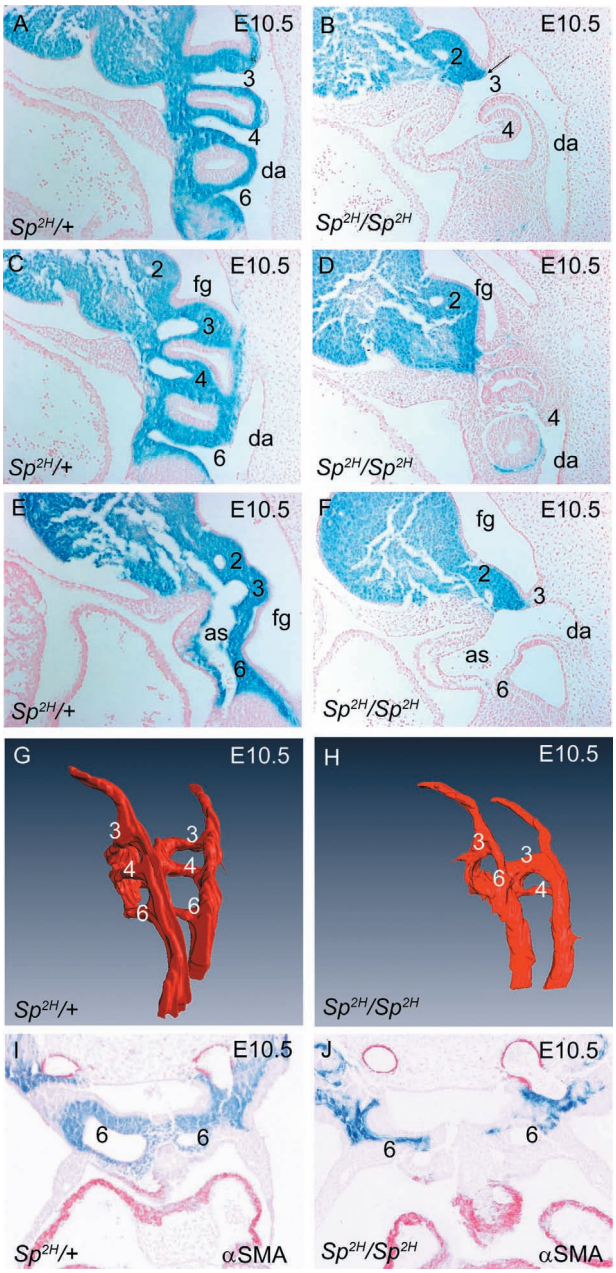

Fig. 2 Posterior arch arteries in *Sp*^{2H} embryos at E10.5. (A–F) Arch arteries 3, 4 and 6 are easily observed in sagittal sections of *Sp*^{2H}/+ embryos and can be seen to connect both with the descending aorta (A) and the aortic sac (E). In *Sp*^{2H}/*Sp*^{2H} embryos, arch artery 3 appears dilated (B,F), whereas arches 4 and 6 are markedly hypoplastic and/or non-patent (D,F). Note that the relationship between the pharyngeal arch arteries and the aortic sac is similar in both *Sp*^{2H}/+ and *Sp*^{2H}/*Sp*^{2H} embryos, showing that caudal movement of the outflow tract had occurred appropriately. (G,H) 3D reconstructions showing the lumens of the posterior pharyngeal arch arteries from *Sp*^{2H}/+ and *Sp*^{2H}/*Sp*^{2H} embryos confirm the hypoplasia of the 4th and 6th arch arteries (in this case, the left 4th and right 6th arches are non-patent in the *Sp*^{2H}/*Sp*^{2H} embryo). (I,J) No αSMA staining was seen surrounding the persistent (*Sp*^{2H}/+) or regressing (*Sp*^{2H}/*Sp*^{2H}) 6th arches at E10.5. as, aortic sac; da, descending aorta; fg, foregut.

majority of cases. This was confirmed both by analysis of transverse sections and three-dimensional reconstructions (Fig. 2G,H). However, a proportion of *Sp*^{2H}/*Sp*^{2H} embryos (20–30% of those examined) had an expanded region in the dorsal wall of the aortic sac, between persisting 4th and 6th arch arteries (Supplementary Fig. 3A). This was despite thinned mesenchyme between the aortic sac and pharynx elsewhere. Notably, the hypoplasia of the 4th and 6th pharyngeal arch arteries seen in the majority of *Sp*^{2H}/*Sp*^{2H} embryos occurred before formation of a smooth muscle layer surrounding the arteries (Fig. 2I,J), suggesting that NCC play a role in stabilization of the nascent vessels, prior to formation of the smooth muscle layer that ensheathes the endothelial tubes.

Deficiency of NCC in the posterior pharyngeal arches prevents initiation of outflow tract septation in *Sp*^{2H}/*Sp*^{2H} embryos

Septation of the distal outflow tract was underway by E11.5 in control embryos when the dorsal wall of the aortic sac fuses with the distal outflow cushions (asterisk, Fig. 3C,I). This fusion confines the flow from the pulmonary channel into the 6th arch arteries and flow from the aortic channel to the 4th arch arteries (Fig. 3A,E). Notably, NCC were abundant in this region, both in the dorsal wall of the aortic sac and in the outflow tract cushions (Fig. 3C,I). The right 4th and 6th arch arteries were obviously beginning to regress by this stage, heralding asymmetrical remodelling of the pharyngeal arch artery system.

Abnormalities in outflow tract development were obvious in each of the six *Sp*^{2H}/*Sp*^{2H} embryos examined at E11.5. Whereas the fusion of the dorsal wall of the aortic sac with the outflow cushions meant that there was no longer an obvious aortic sac in +/+ and *Sp*^{2H}/+ embryos, the dorsal wall of the aortic sac did not fuse with the outflow cushions in the majority (four of six) *Sp*^{2H}/*Sp*^{2H} embryos (double-headed black arrows in Fig. 3D,J) so that the two channels within the outflow tract continued to feed into an enlarged aortic sac before exiting via the 3rd and variably stabilized 4th and 6th pharyngeal arch arteries (Fig. 3B,D,F,H and data not shown). The 3rd pharyngeal arch arteries remained dilated in the *Sp*^{2H}/*Sp*^{2H} embryos, suggesting that they carried the main flow of blood away from the heart (Fig. 3H,J and data not shown). It is likely that these are the *Sp*^{2H}/*Sp*^{2H} embryos that will develop common arterial trunk, which is seen in approximately 75% of *Sp*^{2H}/*Sp*^{2H} embryos in our colony. In the remaining *Sp*^{2H}/*Sp*^{2H} embryos, fusion did occur between the dorsal wall of the aortic sac and the distal outflow cushions, although the morphology was somewhat abnormal (Supplementary Fig. 3B). In these embryos, the left and right 4th and 6th arch arteries were persistent at this stage. It is likely that these are the *Sp*^{2H}/*Sp*^{2H} embryos that develop double outlet right ventricle.

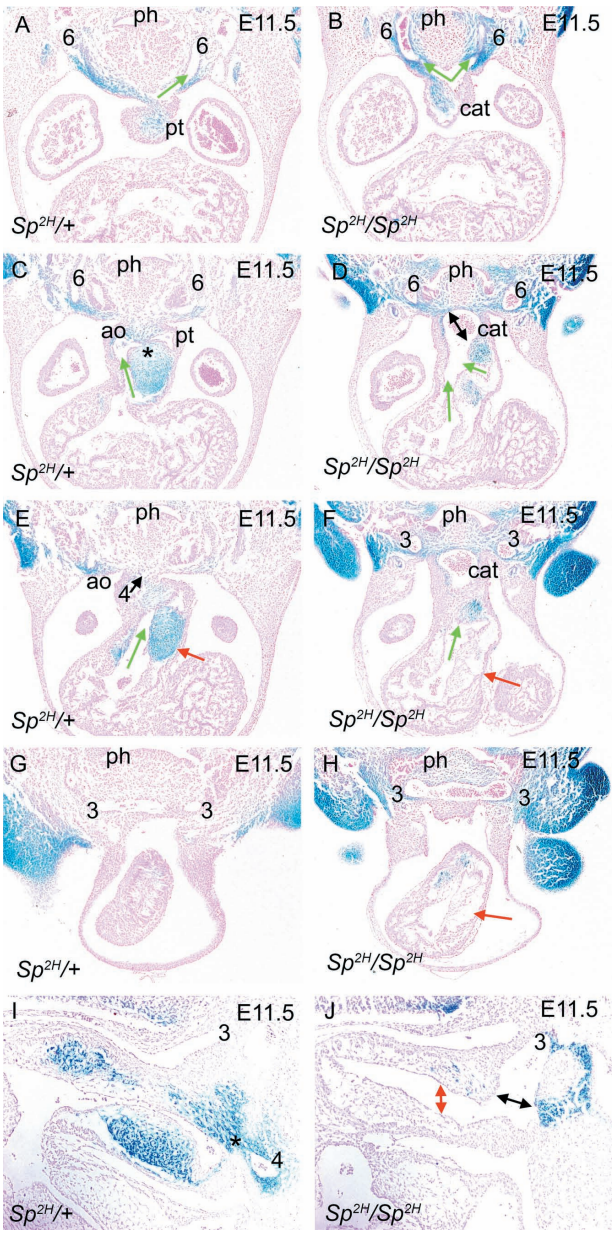

Fig. 3 NCC distribution in Sp^{2H} embryos at E11.5, as outflow tract septation is initiated. In each case, the direction of blood flow through the outflow tract is denoted by green arrows. (A,C,E,G) Transverse sections show that fusion between the dorsal wall of the aortic sac and the distal outflow tract cushions is underway (* in C) in Sp^{2H}/+ embryos, both of which are filled with βgal-expressing NCC. As a consequence, an aortic (green arrow in C) and pulmonary (green arrow in E) channel are apparent in the outflow tract by this stage. The 3rd, 4th and 6th arch arteries are all apparent, although the right 4th and 6th arteries are regressing by this stage. (B,D,F,H) Fusion between the dorsal wall of the aortic sac and the distal outflow cushions does not occur in the Sp^{2H}/Sp^{2H} embryo (double-headed arrow in D). A reduction in the mesenchyme between the pharynx and the aortic sac is still marked in Sp^{2H}/Sp^{2H} embryos. The outflow cushions are deficient in NCC and the proximal regions appear acellular (red arrows in F,H). Despite this, two channels are apparent in the Sp^{2H}/Sp^{2H} outflow tract (green arrows in D). In this embryo, left and right 3rd and 6th arch arteries can be seen, but neither right nor left 4th arch arteries. (I,J) Sagittal sections show the fusion point (asterisk) between the dorsal wall of the aortic sac and the outflow cushions in *Sp2H*/+ embryos (I). In *Sp2H/Sp2H* embryos, the outflow tract cushions are hypoplastic with a marked reduction in βgal-stained cells and there is no fusion with the dorsal wall of the aortic sac (black double-headed arrow in J). The outflow cushions are widely separated (red double-headed arrow in J) and the 3rd arch artery appears dilated. ao, aorta; cat, common arterial trunk; ph, pharynx; pt, pulmonary trunk.

NCC were abundant in the outflow cushions at E11.5 in +/+ and Sp^{2H}/+ embryos, except in the most proximal region. There was a marked reduction in the numbers of NCC in the outflow tract of stage-matched Sp^{2H}/Sp^{2H} embryos, with the cushions appearing acellular in some regions (red arrow in Fig. 3F, compare with Fig. 3E). As a result, the outflow tract cushions were hypoplastic (red arrow in Fig. 3H); this, together with the abnormal positioning of the outflow cushions (compare Fig. 3C,E with Fig. 3D,F; Bajolle et al. 2006), resulted in a failure of the cushions to come together and fuse (red double-headed arrow in Fig. 3J). Similar findings were observed at E12.5 as septation proceeded (Supplementary Fig. 4).

NCC deficiency in the outflow tract cushions does not correlate with the ultimate outflow phenotype in Sp^{2H}/Sp^{2H} fetuses

At E13.5, when outflow tract septation was complete in +/+ and Sp^{2H}/+ fetuses, two distinct outlet phenotypes were easily distinguishable in Sp^{2H}/Sp^{2H} fetuses (Fig. 4D–F and G–I, respectively), as has been described previously (Franz, 1989; Conway et al. 1997a). In the majority (Fig. 4D–F), outflow tract septation had failed completely, resulting in a single outflow vessel (common arterial trunk). In the remainder (Fig. 4G–I), the outflow tract had septated to form the aorta and pulmonary trunk, although both exited from the right ventricle (double outlet right ventricle). Whereas the distal intra-thoracic regions of the great arteries are derived from the left posterior arch arteries, the proximal intra-peritoneal regions are formed by septation of the initially single outflow vessel. In Sp^{2H}/Sp^{2H} fetuses that developed common arterial trunk, the ductus arteriosus was missing in the majority of cases (10 of 11), supporting the data from earlier stages of development that suggested failure to stabilize the 6th arch arteries. In the single case where a ductus arteriosus was present, it was markedly hypoplastic (data not shown). Although NCC were observed in the walls of these vessels, they did not form a continuous lining as they did in the control fetuses (arrowheads in Fig. 4C,F). Moreover, the arch of the aorta was found at a more anterior level in the Sp^{2H}/Sp^{2H} fetuses that developed common arterial trunk (see Fig. 4F, where the aortic arch is seen at the same axial level as the developing mandible) than in those that manifested double outlet right ventricle, or control fetuses. This 'cervical' location of the aortic arch

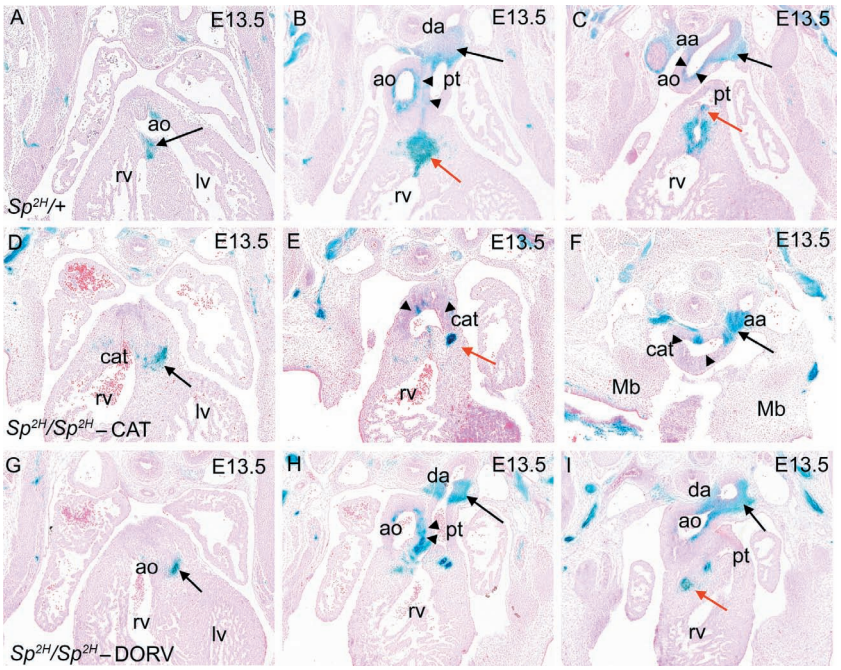

Fig. 4 NCC distribution in Sp^{2H} fetuses at E13.5, after outflow tract septation. (A–C) NCC are found at the fusion point between the outflow cushions and the ventricular septum (arrow in A), the proximal outlet septum (red arrow in B), the great arteries including the walls of the ductus arteriosus (black arrow in B), the aortic arch (black arrow in C) and the separating walls of the aorta and pulmonary trunk (arrowheads in B). βgal-expressing NCC are also found in the pulmonary valves (red arrow in C). (D–F) In Sp^{2H}/Sp^{2H} fetuses with common arterial trunk, NCC are found in the proximal outflow region (arrow in D). Although there are NCC in the aortic arch (arrow in F), there are fewer βgal-expressing NCC in the proximal walls of the common trunk (arrowheads in E and F). A focus of βgal-expressing cells is found in the region where the proximal outlet septum would normally be found (red arrow in E). The aortic arch (F) is seen at the same axial level as the developing mandible, showing its cervical position. (G–I) In Sp^{2H}/Sp^{2H} fetuses with double outlet right ventricle, NCC are found in the proximal outflow region (black arrow in G) and the walls of the great arteries including the ductus arteriosus (black arrow in H), the aortic arch (black arrow in I) and the separating walls of the aorta and pulmonary trunk (arrowheads in H). Although the proximal outlet septum is hypoplastic, a small focus of NCC can be seen (red arrow in I). aa, aortic arch; ao, ascending aorta; cat, common arterial trunk; da, ductus arteriosus; lv, left ventricle; mb, mandible; pt, pulmonary trunk; rv, right ventricle.

supports the idea that it is derived from the 3rd, rather than the 4th, arch artery. Together, these data suggest that there was a close correlation between the maintenance of posterior pharyngeal arch arteries and outflow tract septation.

There was no obvious difference between the Sp^{2H}/Sp^{2H} fetuses that developed double outlet right ventricle and control fetuses in the walls of the great arteries at valve level. However, both had more NCC in this region than those Sp^{2H}/Sp^{2H} fetuses where outflow septation failed, resulting in common arterial trunk (compare arrowheads in Fig. 4B,E,H). Surprisingly, and in contradiction to what has been reported previously (Epstein et al. 2000), we found no obvious differences between the numbers or the pattern of NCC in the most proximal outflow tract of those Sp^{2H}/Sp^{2H} fetuses embryos that developed double outlet right ventricle, compared with those that developed common arterial trunk (Fig. 4D,G). Although the Sp^{2H}/Sp^{2H} fetuses lacked or had hypoplasia of the proximal outlet septum, a smaller but intense focus of NCC was seen in the unfused proximal outflow cushions of Sp^{2H}/Sp^{2H} fetuses (red arrows in Fig. 4B,E,I and Supplementary Fig. 5). These data support those from earlier in gestation, suggesting that it is the presence or absence of NCC in the pharyngeal region, and in regions where the dorsal wall of the aortic sac and proximal outflow cushions fuse, that determines whether the Sp^{2H}/Sp^{2H} fetuses maintain their posterior arch arteries and achieve outflow tract septation, ultimately determining whether the fetuses develop common arterial trunk or double outlet right ventricle.

Abnormalities in Islet1-positive cells in Sp^{2H}/Sp^{2H} embryos

Cells from the SHF add on to the anterior or outflow pole of the mouse heart, contributing to the right ventricle and making an important contribution to the outflow tract (Kelly et al. 2001). These cells are characterized by their expression of the transcriptional regulator *Isl1* (Sun et al. 2007). Cells of SHF origin have been shown to interact with NCC within the pharyngeal region (Vitelli et al. 2002; Moraes et al. 2005). Thus, to determine whether NCC deficiency in the Sp^{2H} mutant resulted in disruption of SHF cells, we used a specific antibody raised against the Isl1 protein (Pfaff et al. 1996).

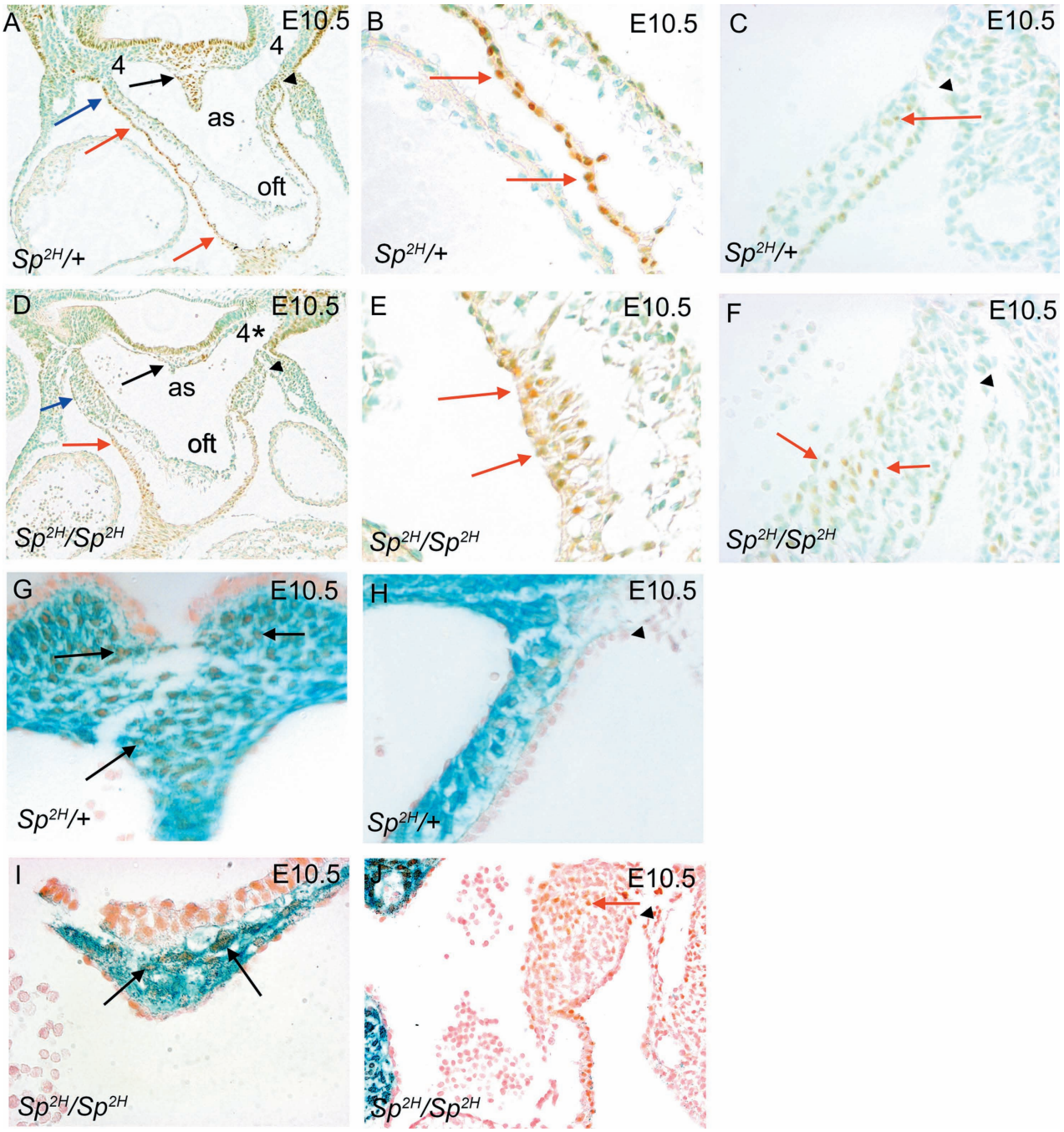

Fig. 5 Isl1 immunostaining of SHF cells and βgal expression by NCC in Sp^{2H} embryos at E10.5. (A–C) The dorsal wall of the aortic sac between the 4th and 6th arch arteries, which will fuse with the distal outflow cushions, is filled with Isl1-expressing cells in Sp^{2H}/+ embryos (black arrow in A). Isl1-immunostained cells are also found in the outer layer of the lateral sides of the aortic sac (blue arrow in A) and in the outflow myocardium (red arrows in A,B), in each case forming a single cell layer. (D–F) In Sp^{2H}/Sp^{2H} embryos, few Isl1-expressing cells can be seen in the dorsal wall of the aortic sac (black arrow in D). Isl1 immunostaining is seen in the lateral sides of the aortic sac (blue arrows in D) and the outflow myocardium (red arrows in D,E). However, the staining in the myocardium reveals that the cells are multilayered (red arrows in E), rather than forming a monolayer as in the Sp^{2H}/+ embryos (red arrows in B). In addition, ectopic Isl1-expressing cells are found in the thickened walls of the aortic sac (red arrows in F). (G,I) NCC and SHF cells are both found in the dorsal wall of the aortic sac, between the origins of the 4th and 6th arch arteries in Sp^{2H}/+ and Sp^{2H}/Sp^{2H} embryos (black arrows), although the numbers of each are much reduced in the hypoplastic structure of the Sp^{2H}/Sp^{2H} embryo. (H,J) Whereas blue-stained NCC are found in the mesenchyme of the aortic sac and distal outflow cushions in Sp^{2H}/+ embryos, they are absent from these latter areas in Sp^{2H}/Sp^{2H} embryos. Ectopic Isl1-expressing SHF cells can be seen in the thickened lateral walls of the aortic sac in Sp^{2H}/Sp^{2H} embryos (red arrow in J). (A,C,D,F,H,J) The black arrowhead marks the pericardial reflections and thus is a landmark which allows comparison between different sections and embryos. as, aortic sac; oft, outflow tract.

Isl1 immunoreactivity was found in restricted domains within the pharyngeal region, including the ventral region of the foregut endoderm and the surface ectoderm of the 2nd pharyngeal pouch, as well as the pharyngeal mesoderm; this latter domain corresponding to the SHF. Isl1 immunostaining was found in the dorsal wall of the aortic sac, localizing to the region between the right and left 3rd , 4th and 6th arch arteries (Supplementary Fig. 6A–C) and the region between the 4th and 6th arch arteries (black arrow in Fig. 5A). Isl1-positive cells were also found in the outer single cell layer of the aortic sac (blue arrow in Fig. 5A) and along the length of the outflow tract (red arrows in Fig. 5A,B). Double labelling for both Isl1 immunoreactivity and Xgal staining of NCC showed that the patterns were complementary throughout most of the pharyngeal region (Supplementary Fig. 6G–I); however, the two cell types were found intermingled in the region of the dorsal wall of the aortic sac, where the 4th and 6th arch arteries separate and where outflow tract septation is initiated (arrows in Fig. 5G).

Analysis of Sp^{2H}/Sp^{2H} embryos demonstrated abundant Isl1-expressing cells, and taking into account the abnormalities in morphology, they followed the same general distribution as in control embryos (Supplementary Fig. 6D–F). However, the region of the dorsal wall of the aortic sac, where the 4th arch arteries would have exited had they been patent, was markedly thinned and contained only a few SHF cells (arrows in Fig. 5I). In addition, there were abnormalities in the distribution of Isl1-positive cells within specific regions of the outflow region. Isl1-positive myocardial cells were found in the thickened walls of the aortic sac of Sp^{2H}/Sp^{2H} embryos and in the adjacent pharyngeal mesenchyme where the 4th arch artery would normally be present (Fig. 5D). The outflow tract myocardium, marked by Isl1-immunoreactivity, also appeared thickened, when compared to the single cell layer observed in the control embryos (compare Fig. 5E with Fig. 5B). Double staining for Isl1 immunoreactivity and βgal-expressing NCC confirmed these data (Supplementary Fig. 6J–L and Fig. 5I,J) and also showed that the ectopic Isl1-positive cells found in the aortic sac of Sp^{2H}/Sp^{2H} embryos were in the region which would normally be filled with NCC (compare Fig. 5J with Fig. 5H), Notably, however, many of the cells in the thickened walls of the aortic sac in Sp^{2H}/Sp^{2H} embryos were negative for both Isl1 and βgal staining. These data suggest that the deficiency of NCC in Sp^{2H} alters the distribution of Isl1-positive cells within the outflow region.

Ectopic myocardial formation in the aortic sac in Sp^{2H}/Sp^{2H} embryos correlates with regions of ectopic Islet1-expressing cells

The SHF cells that contribute to the outflow tract give rise to myocardium and later smooth muscle cells (Waldo et al. 2005b). Having identified abnormalities in SHF addition to

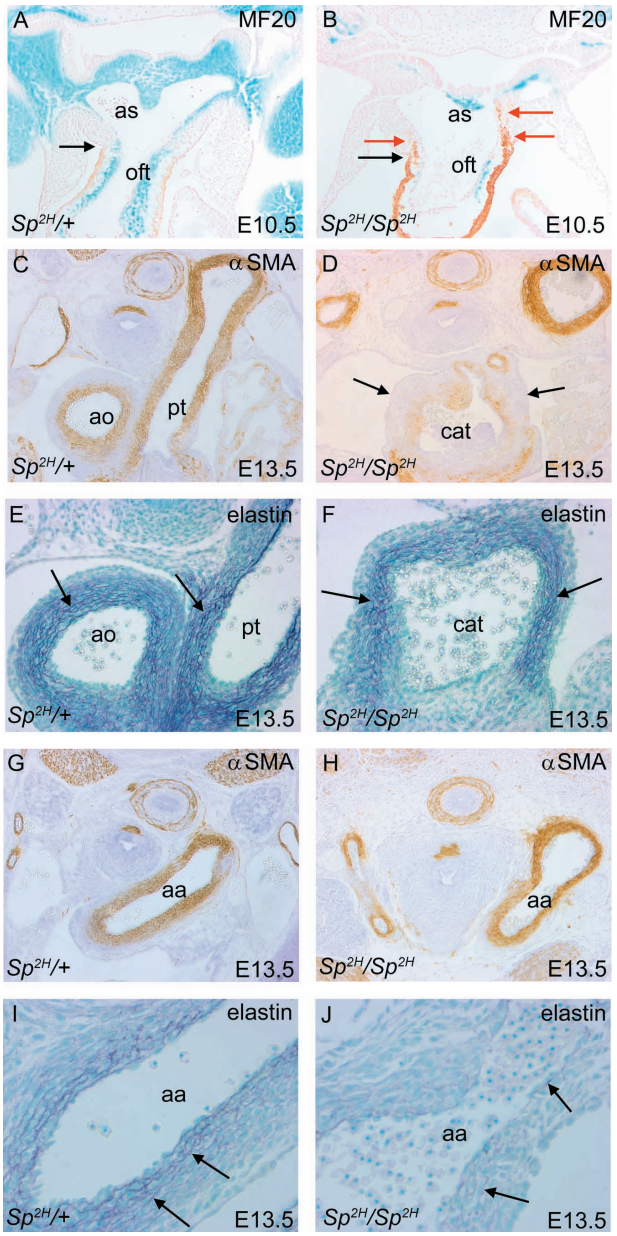

Fig. 6 Formation of myocardium, smooth muscle and an elastic matrix in the outflow vessels of Sp^{2H} embryos and fetuses. (A,B) MF20 labelling of the cardiac muscle (brown) shows that this extends only to the pericardial reflections (arrows in A,B) in $Sp^{2H}/+$ embryos, but ectopically into the aortic sac (red arrows in B) in Sp^{2H}/Sp^{2H} embryos. NCC are marked by their expression of βgal (blue). (C,D,G,H) αSMA immunostaining of E13.5 fetuses shows reduced staining within the arterialized walls of the common trunk in the Sp^{2H}/Sp^{2H} fetus (D) compared with the septated aorta and pulmonary trunk of the $Sp^{2H}/+$ fetus (C). There were similar patterns of staining in the aortic arches of Sp^{2H}/Sp^{2H} embryos and stage matched controls (G,H). (E,F,I,J) Miller's elastin staining of E13.5 fetuses reveals similar patterns of elastin deposition in the proximal region of the arterialized vessels (arrows in E,F), although the layers are more disorganized in the Sp^{2H}/Sp^{2H} fetus. Elastin deposition is much reduced in the aortic arch of Sp^{2H}/Sp^{2H} compared to $Sp^{2H}/+$ fetuses (arrows in I,J). aa, aortic arch; ao, aorta; as, aortic sac; cat, common arterial trunk; oft, outflow tract.

the outflow region in Sp^{2H}, we examined myocardial development of the outflow tract, using MF20, an anti-myosin antibody. In control embryos at E10.5, MF20 staining was found in the outflow tract walls up to the point of the pericardial reflections (black arrows in Fig. 6A,B), but was absent from the adjacent aortic sac (Fig. 6A). In no case was the myocardial marker MF20 found in the dorsal wall of the aortic sac or in the walls of the pharyngeal arch arteries. Examination of Sp^{2H}/Sp^{2H} embryos revealed ectopic expression of MF20 within the aortic sac of Sp^{2H}/Sp^{2H} embryos, in some cases extending into the dorsal region (red arrows in Fig. 6B). Similar, but more extensive, ectopic expression of αSMA was also seen in the lateral walls of the aortic sac (Supplementary Fig. 3B). This suggests that in the situation of neural crest deficiency within the aortic sac, ectopic differentiation of cells of second heart field origin occurs.

Both NCC and SHF cells contribute to the formation of a smooth muscle layer in the great arteries, although within different regions. The smooth muscle cells in the proximal region of the vessels are said to derive from SHF cells. More distally, the smooth muscle cells of the aortic arch derive from NCC, at least in chick (Waldo et al. 2005b). We therefore asked whether smooth muscle cells, and the elastic matrix produced by these cells, are formed normally in Sp^{2H}/Sp^{2H} fetuses and their littermates, at E13.5, the latest stage possible before the intra-uterine death of the Sp^{2H}/Sp^{2H} fetuses. In Sp^{2H}/Sp^{2H} fetuses, αSMA staining was reduced in the most proximal walls of the common trunk (Fig. 6D), although it was well maintained in the aorta and pulmonary trunk in fetuses with double outlet right ventricle (data not shown), as in stage-matched controls. Elastin deposition was found throughout the adventitia of the proximal vessels in the control fetuses and Sp^{2H}/Sp^{2H} (arrows in Fig. 6E,F). Smooth muscle cells were abundant in the aortic arch of control and Sp^{2H}/Sp^{2H} fetuses (Fig. 6G,H), although elastin deposition was markedly reduced in the proximal aortic arch of Sp^{2H}/Sp^{2H} fetuses with common arterial trunk (Fig. 6I,J). These data support the idea that both NCC and SHF populations are disrupted in Sp^{2H}/Sp^{2H} fetuses, and that a combination of these results in the full range of cardiovascular defects seen in this mutant.

Discussion

Splotch is a recognized model of NCC deficiency that has been the subject of several studies (Franz, 1989; Conway et al. 1997b, 2000; Epstein et al. 2000; Chan et al. 2004). However, much of this analysis predates the recognition of the SHF lineage and revision of the segmental heart field model. Moreover, although these studies have shown that NCC are reduced in the pharyngeal and outflow regions, NCC have not been mapped in relationship to the development of the abnormal anatomy of these structures. We have presented data here that suggest that NCC deficiency results in loss of pharyngeal mesenchyme and failure to maintain the posterior arch arteries (4 and 6), which normally form the aortic arch and ductus arteriosus, respectively. In addition, deficiency of NCC in the dorsal wall of the aortic sac and the outflow tract cushions results in a failure of fusion of these structures, preventing the initiation of outflow tract septation. Thus, although deficiency of NCC in the pharyngeal region and outflow tract has been reported previously, our data show for the first time how this deficiency specifically affects the architecture of the distal outflow tract, and why septation defects likely result. Our data also show that the normal distribution of Isl1-expressing cells of SHF origin is dependent on colonization of the pharyngeal and outflow regions by NCC, and that disruption of these SHF cells contributes to the abnormalities observed in Sp^{2H} mutants. Thus, our data give a fresh insight into the requirement for NCC in development of the outflow region of the heart, and highlight the importance of interactions between cells of SHF and neural crest origin in this region. These data also provide an explanation for the cervical aortic arch, common arterial trunk, double outlet right ventricle and absence of ductus arteriosus phenotypes that characterize the Sp^{2H} mutant.

Splotch mice carry mutations in the *Pax3* gene (Epstein et al. 1991), a developmentally regulated transcription factor that is expressed in the dorsal part of the neural tube and early migrating NCC. It has been suggested that the abnormalities in neural crest-derived organs in Sp^{2H} mutants result from defects in the specification or self-renewal of NCC, rather than their migration. Indeed, NCC can migrate long distances in the absence of functional *Pax3*, including the most proximal region of the outflow tract, showing that effects on migration are unlikely to be a major factor in the phenotype (Conway et al. 2000). Although *Pax3* is expressed along the entire neural tube, *Splotch* mice do not have abnormalities in all NCC derivatives. For example, the craniofacial region is well preserved, with abnormalities in the maxilla and mandible seen only rarely, suggesting that *Pax3* may be crucial for local functions or for the specification of subgroups of NCC. This concept is relevant to trying to explain the discrepancy between the marked hypoplasia of the posterior pharyngeal arches, compared with the apparently normal first and second pharyngeal arches (Fig. 1). Epstein et al. (2000) showed, using *Pax3*-Cre, that NCC within the posterior pharyngeal arches are derived from *Pax3*-expressing precursors, whereas those in arches 1 and 2 are not. This suggests that loss of *Pax3* from the precursors of the cells in the posterior pharyngeal arches blocks the formation of NCC that populate the posterior pharyngeal arches, or that abnormal determination affects their pharyngeal arch destination. In support of this, we show in Sp^{2H}/Sp^{2H} embryos at E10.5 a sharp boundary between the NCC-filled 1st and 2nd arches and the posterior 3rd, 4th and 6th pharyngeal arches, which are almost devoid of NCC.

NCC deficiency in *Sp*^{2H} thus results in marked hypoplasia of the posterior pharyngeal arches and loss of their respective arch arteries. NCC have been reported to stabilize the pharyngeal arch arteries in chicken embryos (Bockman et al. 1989, 1990) by ensheathing the newly formed endothelial vessel with mesenchyme which will eventually form smooth muscle cells; in their absence, the nascent artery is rapidly destabilized and lost (Waldo et al. 1996). Our data support a similar mechanism in mouse, in that the 4th and 6th arch arteries are abnormally patterned in *Sp*^{2H}/*Sp*^{2H} embryos before αSMA is apparent in their stage-matched littermates. Thus, in both chicken and mouse, it seems that the loss of NCC-derived mesenchyme within which the vessels form, prevents their stabilization. Recent studies in which NCC are present and patterned apparently normally, but in which the myocardin-related transcription factor B is disrupted, blocking smooth muscle cell differentiation (Li et al. 2005), show that signals for the differentiation of NCC into smooth muscle cells are also crucial for stabilization of the posterior pharyngeal arch arteries. Thus, these data suggest that the ultimate pharyngeal arch artery patterning defects observed in *Sp*^{2H}/*Sp*^{2H} fetuses may result from a combination both of failure of the acellular environment of the hypoplastic posterior arches to support the formation and/or early stabilization of arch arteries 4 and 6, and a role for NCC-derived smooth muscle cells in maintaining these vessels. Disrupted expression of αSMA and elastin in the maturing vessels (at E13.5) of *Sp*^{2H}/*Sp*^{2H} fetuses supports the idea that there is abnormal formation of smooth muscle cells in the situation of NCC deficiency. The absence of 4th and 6th arch arteries in the majority of *Sp*^{2H}/*Sp*^{2H} embryos leads to the left 3rd arch artery becoming dominant, presumably receiving the main flow of blood from the heart and producing the aortic arch at a higher cervical level. The loss of the left 6th arch artery results in the absence of the ductus arteriosus, a crucial component of the normal embryonic pulmonary circulation.

Pharyngeal arch patterning defects, affecting arch arteries 3–6, have been previously reported in *Splotch*^{1H} (Franz, 1989). This mouse line carries the same mutation as the *Splotch*^{2H} mice used here (Beechey & Searle, 1986), although in the case of *Splotch*^{1H} this was always in association with common arterial trunk. Abnormalities in patterning of the posterior pharyngeal arch arteries are also observed in both NCC-ablated chicken embryos. In this case, it was suggested that the aortic sac failed to move caudally with respect to the pharyngeal arch arteries, resulting in their narrowing and consequent abnormal patterning. However, we did not find evidence of impaired caudal movement affecting the outflow tract in *Sp*^{2H}/*Sp*^{2H} embryos compared with their wild type littermates (Fig. 2 and Supplementary Fig. 1). The presence of two distinct outflow phenotypes in our colony, with both common arterial trunk and double outlet right ventricle being found, allows us to draw links between the presence of posterior pharyngeal arch arteries and septation of the outflow tract. In those *Sp*^{2H}/*Sp*^{2H} fetuses that developed common arterial trunk, the left 4th and 6th arch arteries were always absent or severely hypoplastic. In contrast, these arch arteries were maintained, and the dorsal wall of the aortic sac between these arches was able to fuse with the distal outflow cushions thus initiating outflow septation, in *Sp*^{2H}/*Sp*^{2H} fetuses that developed double outlet right ventricle. Whereas the outflow tract can septate in the absence of the 4th pharyngeal arch arteries, for example in *Tbx1*$^{+/-}$ embryos (Liao et al. 2004), the loss of both 6th arch arteries seems to be associated with a failure of septation. Whether this is an incidental finding or closely linked to the failure of septation remains to be established, but the deficiency of NCC in the pharyngeal arches is related to both absence of the 6th arch artery and failure of outflow tract septation. Deficiency of NCC in the dorsal wall of the aortic sac and in the proximal outflow tract cushions results in failure of fusion between these tissues, a process which is essential for the initiation of outflow tract septation. Mesodermal loss of *Tbx1*, using *Mesp1*-Cre, also results in hypoplasia of the posterior pharyngeal arches and common arterial trunk (Zhang et al. 2006). Although *Tbx1* is expressed in non-NCC-derived pharyngeal tissues (Lindsay et al. 2001; Merscher et al. 2001), including those derived from the second heart field (Huynh et al. 2007), in both cases loss of tissue specifically in the region of the dorsal wall of the aortic sac between the origins of the 4th and 6th arch arteries, may prevent the fusion event with the distal outflow cushions that initiates outflow tract septation. The intermingling of NCC and SHF cells (confirmed by *Isl1*-Cre/*ROSA 26R* lineage tracing; our unpublished data) in the dorsal wall of the aortic sac, between the origins of the 4th and 6th arch arteries, compared with the almost mutually exclusive expression patterns found elsewhere in the pharyngeal and outflow regions, suggests that both cell types may be critical to the initiation of outflow tract septation, and moreover, that this may be a key region for interactions between these two cell types. Alternatively, in the absence of 4th and 6th arch arteries, or likely only the 6th, then it may be that septation cannot occur, regardless of the presence or absence of NCC or SHF cells in the aortic sac or outflow tract, as there would be no way for the septated channels to persist without a vessel with which to connect. Whichever hypothesis proves to be correct, this may go some way to explain the similarity in phenotypes observed from loss or deficiency of either cell type.

NCC are also markedly deficient in the outflow tract cushions in *Sp*^{2H}/*Sp*^{2H} embryos. Outflow tract septation occurs in a distal to proximal wave, dependent on the initial fusion event between the distal outflow cushions and the dorsal wall of the aortic sac. More proximally, cushion fusion is essential for the septation and ultimately separation of the aorta from the pulmonary trunk. Hypoplasia of the outflow cushions, resulting from deficiency of NCC, can prevent

the proximal fusion of the cushions even if the initial fusion event takes place. Thus, even in Sp^{2H}/Sp^{2H} fetuses in which the 4th and 6th arch arteries are stabilized and the outflow tract septates (although these fetuses have double outlet right ventricle), there is incomplete fusion of the outflow cushions below valve level.

Sp^{2H}/Sp^{2H} embryos and fetuses have several defects that are indicative of an abnormality in the SHF, including a shortened outflow tract and disrupted formation of smooth muscle in the proximal region of the common arterial trunk. In addition, all of the Sp^{2H}/Sp^{2H} fetuses, whether they develop common arterial trunk or double outlet right ventricle, have their outflow vessels connected to the right ventricle. As alignment of the newly separated aorta and pulmonary trunk with their respective ventricular chambers does not occur until between E12.5 and E13.5 in the developing mouse embryo, the shortened outflow vessel observed at E10.5 in the Sp^{2H}/Sp^{2H} embryos is likely to contribute to the malalignment defects observed later in gestation. Malalignment defects are archetypal of abnormalities in the SHF, and are thought to be related to an abnormality in cardiac looping caused by the shortened outflow tract (Hutson and Kirby, 2003). Indeed, defects in septation and alignment of the outflow tract are observed when several genes essential for formation of the second heart field are disrupted, including *Isl1* and *Tbx20* (Cai et al. 2003; Singh et al. 2005). The close functional relationship between NCC and SHF cells in the outflow region has been demonstrated by NCC ablation in chick embryos (Yelbuz et al. 2002; Waldo et al. 2005a). Rather than migrating into the outflow tract from the SHF, cells proliferated excessively and were displaced to form ectopic myocardium in abnormal bulges of the neural crest-ablated aortic sac (Waldo et al. 2005a). Our analysis of Isl1-positive SHF cells in the pharyngeal and outflow region supports the idea that the cells originating in the SHF are disrupted by the deficiency in NCC in Sp^{2H}/Sp^{2H} embryos. As in the chicken, we saw displacement of cells of SHF origin into bulges found in the distal outflow tract, where they formed cardiomyocytes and smooth muscle cells. Moreover, the Isl1-positive walls of the outflow tract were thickened, resembling cells undergoing the process of myocardialization where the muscle cells migrate into the outflow tract cushions (Van den Hoff et al. 1999; Phillips et al. 2005). As these myocardializing cells are known to be SHF-derived (Sun et al. 2007), this suggests that the deficiency of NCC within the outflow cushions may be inducing this process prematurely.

Surprisingly, although NCC- and Isl1-expressing cells were generally complementary throughout the pharyngeal and outflow region, βgal attaining of NCC and Isl1 immunoreactivity were both found in the central region of the dorsal wall of the aortic sac between the 4th and 6th pharyngeal arch arteries. Although it is difficult to distinguish between co-expression of these markers by a single cell type vs. intermingling of cells expressing a single marker, the latter seems more likely. Isl1 is expressed by some neurones, such as those within the sympathetic ganglia (see Supplementary Fig. 6A). However, in our previous analysis of the innervation of the heart (Hildreth et al. 2008) we did not observe neurones in the dorsal wall of the aortic sac at this stage of development. Thus, we conclude that SHF-derived cells and NCC are both found in the region of the dorsal of wall of the aortic sac which fuses with the distal outflow cushions. This, in combination with the requirement for both cell types in the normal patterning of the posterior pharyngeal arch arteries, may go some way to explain why deficiencies in each population cause similar outflow defects.

Together, our data show that NCC play essential roles in outflow tract septation; forming pharyngeal mesenchyme which is required for the normal architecture of the aortic sac, stabilizing the posterior arch arteries in the pharyngeal region and forming the mesenchyme of the outflow tract cushions. In addition, the NCC influence the cells from the SHF, perhaps contributing to the overall cardiovascular phenotype observed in Sp^{2H}/Sp^{2H} fetuses. Unravelling the relationship between these two cell types is likely to be of major importance in understanding the aetiology of malformations affecting the outflow region in humans.

Acknowledgement

This project was supported in its entirety by funding from the British Heart Foundation.

References

Bajolle F, Zaffran S, Kelly RG, et al. (2006) Rotation of the myocardial wall of the outflow tract is implicated in the normal positioning of the great arteries. *Circ Res* **98**, 421–428.

Bartelings MM, Gittenberger-de Groot AC (1989) The outflow tract of the heart – embryologic and morphologic correlations. *Int J Cardiol* **22**, 289–300.

Beechey CV, Searle AG (1986) Mutations at the Sp locus. *Mouse News Lett* **75**, 28.

Bernanke DH, Markwald RR (1982) Migratory behavior of cardiac cushion tissue cells in a collagen-lattice culture system. *Dev Biol* **91**, 235–245.

Bockman DE, Redmond ME, Kirby ML (1989) Alteration of early vascular development after ablation of cranial neural crest. *Anat Rec* **225**, 209–217.

Bockman DE, Redmond ME, Kirby ML (1990) Altered development of pharyngeal arch vessels after neural crest ablation. *Ann N Y Acad Sci* **588**, 296–304.

Cai CL, Liang X, Shi Y, et al. (2003) Isl1 identifies a cardiac progenitor population that proliferates prior to differentiation and contributes a majority of cells to the heart. *Dev Cell* **5**, 877–889.

Chan WY, Cheung CS, Yung KM, Copp AJ (2004) Cardiac neural crest of the mouse embryo: axial level of origin, migratory pathway and cell autonomy of the splotch (Sp2H) mutant effect. *Development* **131**, 3367–3379.

Conway SJ, Henderson DJ, Kirby ML, Anderson RH, Copp AJ (1997a) Development of a lethal congenital heart defect in the splotch (Pax3) mutant mouse. *Cardiovasc Res* **36**, 163–173.

Conway SJ, Henderson DJ, Copp AJ (1997b) Pax3 is required for cardiac neural crest migration in the mouse: evidence from the splotch (Sp2H) mutant. *Development* **124**, 505–514.

Conway SJ, Bundy J, Chen J, Dickman E, Rogers R, Will BM (2000) Decreased neural crest stem cell expansion is responsible for the conotruncal heart defects within the splotch (Sp(2H))/Pax3 mouse mutant. *Cardiovasc Res* **47**, 314–328.

Danielian PS, Muccino D, Rowitch DH, Michael SK, McMahon AP (1998) Modification of gene activity in mouse embryos in utero by a tamoxifen inducible form of Cre recombinase. *Curr Biol* **8**, 1323–1326.

Epstein DJ, Vekemans M, Gros P (1991) Splotch (Sp2H), mutation affecting development of the mouse neural tube, shows a deletion within the paired homeodomain of Pax-3. *Cell* **67**, 767–774.

Epstein JA, Li J, Lang D, et al. (2000) Migration of cardiac neural crest cells in Splotch embryos. *Development* **127**, 1869–1878.

Franz T (1989) Persistent truncus arteriosus in the Splotch mutant mouse. *Anat Embryol (Berl)* **180**, 457–464.

Henderson DJ, Conway SJ, Copp AJ (1999) Rib truncations and fusions in the Sp2H mouse reveal a role for Pax3 in specification of the ventro-lateral and posterior parts of the somite. *Dev Biol* **209**, 143–158.

Hildreth V, Webb S, Bradshaw L, Brown NA, Anderson RH, Henderson DJ (2008) Jan cells migrating from the neural crest contribute to the innervation of the venous pole of the heart. *J Anat* **212**, 1–11.

Hutson MR, Kirby ML (2003) Neural crest and cardiovascular development: a 20-year perspective. *Birth Defects Res C Embryo Today* **69**, 2–13.

Hutson MR, Kirby ML (2007) Model systems for the study of heart development and disease. Cardiac neural crest and conotruncal malformations. *Semin Cell Dev Biol* **18**, 101–110.

Huynh T, Chen L, Terrell P, Baldini A (2007) A fate map of Tbx1 expressing cells reveals heterogeneity in the second cardiac field. *Gene* **45**, 470–475.

Icardo JM (1990) Development of the outflow tract. A study in hearts with situs solitus and situs inversus. *Ann N Y Acad Sci* **588**, 26–40.

Jiang X, Rowitch DH, Soriano P, McMahon AP, Sucov HM (2000) Fate of the mammalian cardiac neural crest. *Development* **127**, 1607–1616.

Kelly RG, Brown NA, Buckingham ME (2001) The arterial pole of the mouse heart forms from Fgf10-expressing cells in pharyngeal mesoderm. *Dev Cell* **1**, 435–440.

Kirby ML, Gale TF, Stewart DE (1983) Neutral crest cells contribute to normal aorticopulmonary septation. *Science* **220**, 1059–1061.

Li J, Zhu X, Chen M, et al. (2005) Myocardin-related transcription factor B is required in cardiac neural crest for smooth muscle differentiation and cardiovascular development. *Proc Natl Acad Sci USA* **102**, 8916–8921.

Liao J, Kochilas L, Nowotschin S, et al. (2004) Full spectrum of malformations in velo-cardio-facial syndrome/DiGeorge syndrome mouse models by altering Tbx1 dosage. *Hum Mol Genet* **13**, 1577–1585.

Lincoln J, Alfieri CM, Yutzey KE (2004) Development of heart valve leaflets and supporting apparatus in chicken and mouse embryos. *Dev Dyn* **230**, 239–250.

Lindsay EA, Vitelli F, Su H, et al. (2001) Tbx1 haploinsufficiency in the DiGeorge syndrome region causes aortic arch defects in mice. *Nature* **410**, 97–101.

Loughna S, Henderson D (2007) Methodologies for staining and visualisation of β-galactosidase in mouse embryos and tissues. In *Reporter Genes. Methods in Molecular Biology series* (eds Donald S. Anson), pp. 1–11. Totowa, New Jersey: Humana Press.

Merscher S, Funke B, Epstein JA, et al. (2001) TBX1 is responsible for cardiovascular defects in velo-cardio facial/DiGeorge syndrome. *Cell* **104**, 619–629.

Mjaatvedt CH, Nakaoka T, Moreno-Rodriguez R, et al. (2001) The outflow tract of the heart is recruited from a novel heart-forming field. *Dev Biol* **238**, 97–109.

Moraes F, Novoa A, Jerome-Majewska LA, Papaioannou VE, Mallo M (2005) Tbx1 is required for proper neural crest migration and to stabilize spatial patterns during middle and inner ear development. *Mech Dev* **122**, 199–212.

Pfaff SL, Mendelsohn M, Stewart CL, Edlund T, Jessell TM (1996) Requirement for LIM homeobox gene Isl1 in motor neuron generation reveals a motor neuron-dependent step in interneuron differentiation. *Cell* **84**, 309–320.

Phillips HM, Murdoch JN, Chaudhry B, Copp AJ, Henderson DJ (2005) Vangl2 acts via RhoA signaling to regulate polarized cell movements during development of the proximal outflow tract. *Circ Res* **96**, 292–299.

Singh MK, Christoffels VM, Dias JM, et al. (2005) Tbx20 is essential for cardiac chamber differentiation and repression of Tbx2. *Development* **132**, 2697–2707.

Soriano P (1999) Generalized lacZ expression with the ROSA26 Cre reporter strain. *Nat Genet* **21**, 70–71.

Sun Y, Liang X, Najafi N, et al. (2007) Islet 1 is expressed in distinct cardiovascular lineages, including pacemaker and coronary vascular cells. *Dev Biol* **304**, 286–296.

van den Hoff MJ, Moorman AF, Ruijter JM, et al. (1999) Myocardialization of the cardiac outflow tract. *Dev Biol* **212**, 477–490.

Vitelli F, Morishima M, Taddei I, Lindsay EA, Baldini A (2002) Tbx1 mutation causes multiple cardiovascular defects and disrupts neural crest and cranial nerve migratory pathways. *Hum Mol Genet* **11**, 915–922.

Waldo KL, Kumiski D, Kirby ML (1996) Cardiac neural crest is essential for the persistence rather than the formation of an arch artery. *Dev Dyn* **205**, 281–292.

Waldo KL, Kumiski DH, Wallis KT, et al. (2001) Conotruncal myocardium arises from a secondary heart field. *Development* **128**, 3179–3188.

Waldo KL, Hutson MR, Stadt HA, Zdanowicz M, Zdanowicz J, Kirby ML (2005a) Cardiac neural crest is necessary for normal addition of the myocardium to the arterial pole from the secondary heart field. *Dev Biol* **281**, 66–77.

Waldo KL, Hutson MR, Ward CC, et al. (2005b) Secondary heart field contributes myocardium and smooth muscle to the arterial pole of the developing heart. *Dev Biol* **281**, 78–90.

Webb S, Qayyum SR, Anderson RH, Lamers WH, Richardson MK (2003) Septation and separation within the outflow tract of the developing heart. *J Anat* **202**, 327–342.

Xu H, Morishima M, Wylie JN, et al. (2004) Tbx1 has a dual role in the morphogenesis of the cardiac outflow tract. *Development* **131**, 3217–3227.

Yelbuz TM, Waldo KL, Kumiski DH, Stadt HA, Wolfe RR, Leatherbury L, Kirby ML (2002) Shortened outflow tract leads to altered cardiac looping after neural crest ablation. *Circulation* **106**, 504–510.

Zhang Z, Huynh T, Baldini A (2006) Mesodermal expression of Tbx1 is necessary and sufficient for pharyngeal arch and cardiac outflow tract development. *Development* **133**, 3587–3595.

Supporting Information

Additional Supporting Information may be found in the online version of this article:

Fig. S1 Sagittal sections showing NCC distribution at E10.5. (A–D) Sagittal sections show that NCC are abundant in the mesenchyme between the dorsal wall of the aortic sac and the foregut (black arrows in C), the outflow cushions (red arrows in C) and surround the posterior pharyngeal arch arteries (A) in Sp^{2H}/+ embryos. In Sp^{2H}/Sp^{2H} embryos there is a demarcation of NCC at the 2nd pharyngeal pouch (red arrow in B). Consequently, there are very few NCC in the dorsal wall of the aortic sac (black arrows in D) and the outflow cushions (red arrow in D) and the posterior arch arteries are not surrounded by NCC, with only small isolated clumps of blue-stained cells visible (arrowheads in B,D). as, aortic sac; fg, foregut; oft, outflow tract.

Fig. S2 Proliferation and programmed cell death in Sp^{2H}/Sp^{2H} embryos at E10.5. There are no apparent differences in either proliferation (A,B) or apoptosis (C,D) in Sp^{2H}/Sp^{2H} embryos compared to their stage-matched littermates.

Fig. S3 Morphology of the distal outflow tract in Sp^{2H}/Sp^{2H} embryos likely to develop double outlet right ventricle. (A) Although the dorsal wall of the aortic sac is thinned in this Sp^{2H}/Sp^{2H} embryo at E10.5, with little mesenchyme separating the aortic sac from the pharynx, the region between the persisting 4th and 6th arch arteries, corresponding to the dorsal wall of the aortic sac, is well developed (arrow). (B) A similar morphology is seen in an Sp^{2H}/Sp^{2H} embryo at E11.5. Again, the 4th arch arteries are persisting and it seems likely that the dorsal wall of the aortic sac (arrow) will fuse with the outflow cushions. NCC (blue) are deficient, however, with only a very few cells seen in the outflow cushions (arrowhead). Note that ectopic αSMA staining is seen in the mesenchyme of the aortic sac (red arrows).

Fig. S4 Outflow morphology at E12.5 in Sp^{2H}/Sp^{2H} embryos. Similar to E11.5 and E13.5, the outflow tract remains unseptated in the majority of Sp^{2H}/Sp^{2H} embryos at E12.5, with a reduction in the numbers of NCC seen.

Fig. S5 Sagittal sections showing NCC distribution in Sp^{2H} fetuses at E13.5. Deficiency in NCC is particularly apparent in the developing sub-pulmonary infundibulum (red arrow B,E). Green arrows in A, C and D denote direction of blood flow through the ductus arteriosus, aorta and common arterial trunk, respectively. ao, aorta; cat, common arterial trunk; da, ductus arteriosus; dao, descending aorta; ivs, interventricular septum; lv, left ventricle; pt, pulmonary trunk; rv, right ventricle.

Fig. S6 Isl1 immunostaining of SHF cells and βgal expression by NCC in Sp^{2H} embryos at E10.5. (A–C) Isl1 immunostaining (brown) is found in the separating walls between the left and right 3rd (A), 4th (B) and 6th (C) arch arteries in Sp^{2H}/+ embryos, in continuity with the walls of the outflow tract. (D–F) The same distribution is found in Sp^{2H}/Sp^{2H} embryos, except that as the 4th arches are non-patent (4* in E). The pharyngeal mesenchyme is markedly deficient between the foregut and the dorsal wall of the aortic sac (arrowheads in E) and very little Isl1 immunostaining can be seen in this region. (G–L) βgal-stained NCC (blue) and Isl1 immunostained SHF cells (brown) generally show complementary expression patterns in the pharyngeal arches and outflow region in both Sp^{2H}/+ and Sp^{2H}/Sp^{2H} embryos. sg, sympathetic ganglia.

Please note: Wiley-Blackwell are not responsible for the content or functionality of any supporting materials supplied by the authors. Any queries (other than missing material) should be directed to the corresponding author for the article.